Effects of strong magnetic fields in strange baryonic matter

A.E. Broderick [a], M. Prakash [b], J.M. Lattimer [b]

[a] *Theoretical Astrophysics, California Institute of Technology, 1200 East California Blvd, Pasadena, CA 91125, USA*
[b] *Department of Physics and Astronomy, State University of New York at Stony Brook, Stony Brook, NY 11974-3800, USA*

Abstract

We investigate the effects of very strong magnetic fields upon the equation of state of dense baryonic matter in which hyperons are present. In the presence of a magnetic field, the equation of state above nuclear density is significantly affected both by Landau quantization and magnetic moment interactions, but only for field strengths $B > 5 \times 10^{18}$ G. The former tends to soften the EOS and increase proton and lepton abundances, while the latter produces an overall stiffening of the EOS. Each results in a suppression of hyperons relative to the field-free case. The structure of a neutron star is, however, primarily determined by the magnetic field stress. We utilize existing general relativistic magneto-hydrostatic calculations to demonstrate that maximum average fields within a stable neutron are limited to values $B \leqslant 1$–3×10^{18} G. This is not large enough to significantly influence particle compositions or the matter pressure, unless fluctuations dominate the average field strengths in the interior or configurations with significantly larger field gradients are considered.

Recent discoveries that link soft γ-ray repeaters and perhaps some anomalous X-ray pulsars with neutron stars having ultrastrong magnetic fields—the so-called magnetars (see Table 1 in [1] for a summary)—have spurred theoretical studies of the effects ultrastrong magnetic fields have on the equation of state (EOS) of neutron-star matter and on the structure of neutron stars (cf. [1–3] and references therein). The magnetic field strength B needed to dramatically affect neutron star structure directly can be estimated with a dimensional analysis [4] equating the magnetic

field energy $E_B \sim (4\pi R^3/3)(B^2/8\pi)$ with the gravitational binding energy $E_{\text{B.E.}} \sim 3\,GM^2/5R$, yielding

$$B \sim 1.4 \times 10^{18}\left(\frac{M}{1.4\,M_\odot}\right)\left(\frac{R}{10\text{ km}}\right)^{-2}\text{ G}, \qquad (1)$$

where M and R are, respectively, the neutron star mass and radius.

To date, studies of the effects of such ultrastrong magnetic fields on the EOS and on the structure of neutron stars have been largely limited to cases in which the strongly interacting component of matter is comprised of nucleons [3,5–7]. Our objective in this Letter is to investigate the effects of magnetic fields on the EOS of matter containing strangeness-bearing hyperons. Towards this end, we utilize the theoret-

E-mail addresses: aeb@tapir.caltech.edu (A.E. Broderick),
prakash@snare.physics.sunysb.edu (M. Prakash),
lattimer@astro.sunysb.edu (J.M. Lattimer).

Table 1
The measured magnetic moments of spin-$\frac{1}{2}$ baryons from Ref. [8]. $\mu_N = e\hbar/(2m_p) = 3.15 \times 10^{-18}$ MeV G^{-1} is the nuclear magneton and the anomalous magnetic moment $\kappa_b = (\mu_b/\mu_N - q_b m_p/m_b)\,\mu_N$

Species b	Mass (MeV)	Charge q_b	Magnetic moment μ_b/μ_N	Anomalous moment κ_b/μ_N
p	938.3	1	2.79	1.79
n	939.6	0	-1.91	-1.91
Λ	1115.7	0	-0.61	-0.61
Σ^+	1189.4	1	2.46	1.67
Σ^0	1192.6	0	1.61	1.61
Σ^-	1197.4	-1	-1.16	-0.38
Ξ^0	1314.9	0	-1.25	-1.25
Ξ^-	1321.3	-1	-0.65	0.06

ical formalism for the EOS developed in Ref. [3]. This allows us to consistently incorporate the effects of magnetic fields on the EOS in multicomponent, interacting matter. For the first time, the anomalous magnetic moments of baryons is included, using a covariant description. A further objective is to explore the consequences of strong magnetic fields for neutron star structure and maximum masses, which is accomplished using the results of general relativistic structural calulations in Ref. [1].

Charge neutral, beta-equilibrated, neutron-star matter contains both negatively charged leptons (e and μ) and positively charged baryons (p and, at higher densities, Σ^+). Magnetic fields quantize the orbital motion (Landau quantization) of these charged particles. When the Fermi energy of the p or Σ^+ becomes significantly altered by the magnetic field, the pressure and composition of matter in beta equilibrium are affected. Landau quantization has a significant effect when $B^* = B/B_c^e \sim 10^5$ ($B_c^e = \hbar c/(e\lambdabar_e^2) = 4.414 \times 10^{13}$ G is the critical electron field) [3,5–7]. Higher fields lead to a general softening of the EOS relative to the case in which magnetic fields are absent.

In strong magnetic fields, contributions from the anomalous magnetic moments of the baryons (denoted hereafter by κ_b) must also be considered. The measured magnetic moments μ_b for nucleons and strangeness-bearing hyperons are given in Table 1. With few exceptions, the anomalous magnetic moments are similar in magnitude. As discussed below, the energies $|\kappa_n B| \simeq 2.7 \times 10^{-4} B^*$ MeV and $|\kappa_p B| \simeq 2.5 \times 10^{-4} B^*$ MeV measure the changes to the nucleon Fermi energies, and $|\kappa_n + \kappa_p| B \simeq 1.67 \times 10^{-5} B^*$ MeV measures the change to the beta equi-

librium condition. Since the Fermi energies exceed 20 MeV for the densities of interest, it is clear that contributions from the anomalous magnetic moments become significant for $B^* > 10^5$. For such large fields, complete spin polarization of the neutrons occurs, producing an increase in degeneracy pressure and an overall stiffening of the EOS that overwhelms the softening induced by Landau quantization [3].

Similary, in the presence of strong magnetic fields, all of the hyperons are susceptible to spin polarization due to magnetic moment interactions with the field. The net result of the opposing effects of degeneracy and Landau quantization will depend on the relative concentrations of the various hyperons, which in turn depend sensitively on the hyperon–meson interactions for which only a modest amount of guidance is available [9–11]. It is one of the purposes of this work to ascertain the influence of feedback effects due to mass and energy shifts in multi-component matter.

To describe the EOS of neutron-star matter, we employ a field theoretical approach (at the mean field level) in which the baryons interact via the exchange of σ–ω–ρ mesons.[1] We consider two classes of models that differ in their high density behavior. The two Lagrangian densities are given by [12,13]

$$\mathcal{L}_{\mathrm{I}} = \mathcal{L}_b - \left(1 - \frac{g_{\sigma b}\sigma}{m_b}\right)\overline{\Psi}_b m_b \Psi_b + \mathcal{L}_m + \mathcal{L}_\ell,$$

---

[1] The qualitative effects of strong magnetic fields found in the field-theoretical models also exist in non-relativistic potential models. This is because the phase space of charged particles is similarly affected in both approaches by magnetic fields. The effects due to the anomalous magnetic moments would, however, enter linearly in a non-relativistic approach, and would thus be more dramatic in that case.

Table 2
Nucleon–meson and hyperon–meson coupling constants for the GM1–3 and ZM models. The hyperon to nucleon coupling ratios were taken from Ref. [16]

Model	$g_{\sigma N}/m_\sigma$ (fm)	$g_{\omega N}/m_\omega$ (fm)	$g_{\rho N}/m_\rho$ (fm)	$x_{\sigma H}$	$x_{\omega H}$	$x_{\rho H}$	b	c
GM1	3.434	2.674	2.100	0.6	0.653	0.6	0.002947	−0.001070
GM2	3.025	2.195	2.189	0.6	0.659	0.6	0.003478	0.01328
GM3	3.151	2.195	2.189	0.6	0.659	0.6	0.008659	−0.002421
ZM	2.736	1.617	2.185	1.0	1.0	1.0	0.0	0.0

Table 3
Nuclear matter properties used to fit coupling constants for the GM1–3 Glendenning and Moszkowski (GM1–3) Zimanyi and Moszkowski (ZM) models

Model	n_s (fm^{-3})	$-B/A$ (MeV)	M^*/M	K_0 (MeV)	$a_{\rm sym}$ (MeV)
GM1	0.153	16.30	0.70	300	32.5
GM2	0.153	16.30	0.78	300	32.5
GM3	0.153	16.30	0.78	240	32.5
ZM	0.160	16.00	0.86	225	32.5

$$\mathcal{L}_{\rm II} = \left(1 + \frac{g_{\sigma b}\sigma}{m_b}\right)\mathcal{L}_b - \overline{\Psi}_b m_b \Psi_b + \mathcal{L}_m + \mathcal{L}_\ell. \qquad (2)$$

The baryon, lepton, and meson Lagrangians are given by

$$\mathcal{L}_b = \overline{\Psi}_b\big(i\gamma_\mu\partial^\mu + q_b\gamma_\mu A^\mu - g_{\omega b}\gamma_\mu\omega^\mu$$
$$- g_{\rho b}\tau_{3_b}\gamma_\mu\rho^\mu - \kappa_b\sigma_{\mu\nu}F^{\mu\nu}\big)\Psi_b,$$

$$\mathcal{L}_\ell = \overline{\psi}_l\big(i\gamma_\mu\partial^\mu + q_l\gamma_\mu A^\mu\big)\psi_l \quad \text{and}$$

$$\mathcal{L}_m = \frac{1}{2}\partial_\mu\sigma\,\partial^\mu\sigma - \frac{1}{2}m_\sigma^2\sigma^2 - U(\sigma) + \frac{1}{2}m_\omega^2\omega_\mu\omega^\mu$$
$$- \frac{1}{4}\Omega^{\mu\nu}\Omega_{\mu\nu} + \frac{1}{2}m_\rho^2\rho_\mu\rho^\mu$$
$$- \frac{1}{4}P^{\mu\nu}P_{\mu\nu} - \frac{1}{4}F^{\mu\nu}F_{\mu\nu}, \qquad (3)$$

where Ψ_b and ψ_ℓ are the baryon and lepton Dirac fields, respectively. The index b runs over the baryons n, p, Λ, Σ^-, Σ^0, Σ^+, Ξ^-, and Ξ^0. (Neglect of the Ω^- and the Δ quartet, which appear only at very high densities, does not qualitatively affect our conclusions.) The index ℓ runs over the electron and muon. The baryon mass and the isospin projection are denoted by m_b and τ_{3_b}, respectively. The mesonic and electromagnetic field tensors are given by their usual expressions: $\Omega_{\mu\nu} = \partial_\mu\omega_\nu - \partial_\nu\omega_\mu$, $P_{\mu\nu} = \partial_\mu\rho_\nu - \partial_\nu\rho_\mu$, and $F_{\mu\nu} = \partial_\mu A_\nu - \partial_\nu A_\mu$. The strong interaction couplings are denoted by g, the electromagnetic couplings by q, and the meson masses by m all with ap-

propriate subscripts. The quantity $U(\sigma)$ denotes scalar self-interactions and is taken to be of the form $U(\sigma) = (bm_n/3)(g_{\sigma N}\sigma)^3 + (c/4)(g_{\sigma N}\sigma)^4$ [12,14,15].

The anomalous magnetic moments are introduced via the minimal coupling of the baryons to the electromagnetic field tensor for each baryon. Their contributions in the Lagrangian are contained in the term $-\kappa_b\overline{\Psi}_b\sigma_{\mu\nu}F^{\mu\nu}\Psi_b$, where $\sigma_{\mu\nu} = \frac{i}{2}[\gamma_\mu, \gamma_\nu]$. Although the electromagnetic field is included in $\mathcal{L}_{\rm I}$ and $\mathcal{L}_{\rm II}$, it assumed to be externally generated and only frozen-field configurations will be considered.

The meson–nucleon g_{iN} ($i = \sigma, \omega, \rho$), and scalar self-interaction couplings, b and c, were chosen to reproduce the binding energy B/A, the nuclear saturation density n_s, the Dirac effective mass M^*, and the symmetry energy a_s. The values of the couplings used in the models considered are shown in Table 2, and the associated nuclear matter properties used to calculate these couplings are shown in Table 3.

The meson–hyperon couplings are assumed to be fixed fractions of the meson–nucleon couplings, i.e., $g_{iH} = x_{iH}g_{iN}$, where for each meson i, the values of x_{iH} are assumed equal for all hyperons H. The values of x_{iH} are chosen to reproduce the binding energy of the Λ at nuclear saturation as suggested by Glendenning and Moszkowski (GM) [9] and are also given in Table 2. The high-density behavior of the EOS is sensitive to the strength of the meson couplings

employed [10] and the models chosen encompass a fairly wide range of variation. Models GM1–3 employ linear scalar couplings ($\mathcal{L}_{\mathrm{I}}$), while the Zimanyi and Moszkowski (ZM) model employs a nonlinear scalar coupling ($\mathcal{L}_{\mathrm{II}}$), which is reflected in the high density behaviors of m_n^*/m_n. Comparison of results from the GM1–3 and ZM models allows us to contrast the effects of the underlying EOS.

The field equations (not explicitly displayed here) follow from a natural extension of those used in Ref. [3] to the case in which hyperons are present. In charge neutral and beta equilibrated matter, the conditions

$$\sum_b q_b n_b + \sum_l q_l n_l = 0 \quad \text{and}$$

$$\mu_b = B_b \mu_n - q_b \mu_e, \tag{4}$$

where μ_b is the baryon chemical potential (not to be confused with the magnetic moment μ_b of Table 1)

and B_b is the baryon number, also apply. The energy spectra, number densities, scalar number densities, energy densities, and total pressure are given by straightforward generalizations of their analogues in Ref. [3].

In Fig. 1, results are shown for physical quantities of interest for the baseline model GM3, when the effects of Landau quantization are included but those of anomalous magnetic moments are ignored. As the magnetic field is varied, the generic behavior of the matter pressure P_m, effective neutron mass m_n^*, and particle abundances are the same as those found in Ref. [3], in which matter containing only nucleons was considered. When hyperons appear, the pressure becomes smaller than the case of pure nucleons for all fields. The effective nucleon mass decreases slightly when hyperons appear, again independently of the field strength. The appearance of hyperons produces pronounced effects on the nucleon and lepton abundances.
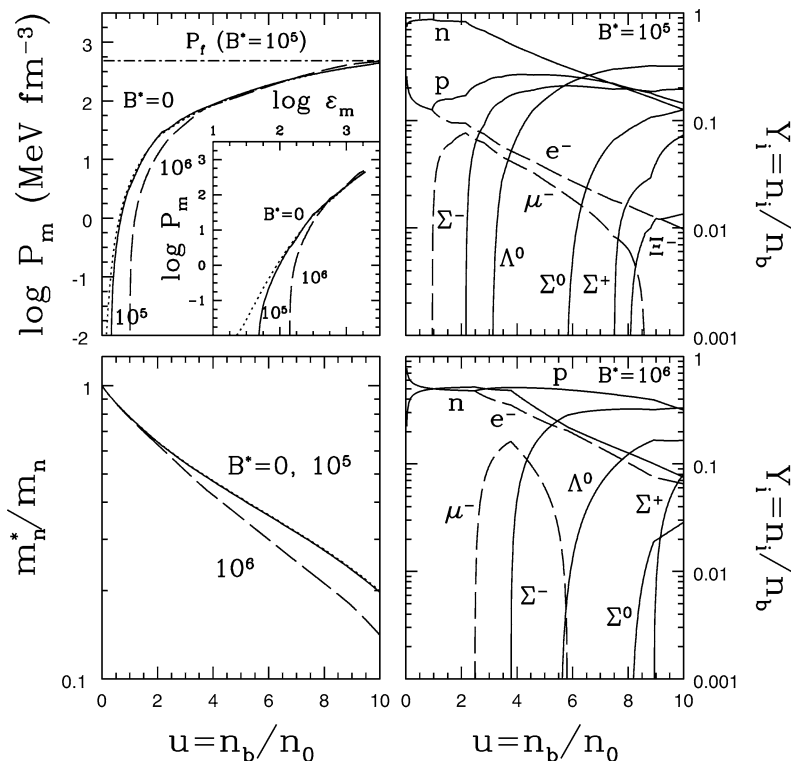

Fig. 1. Matter pressure P_m, neutron Dirac effective mass m_n^*/m_n, and concentrations Y_i as functions of density ($n_0 = 0.16$ fm^{-3} is the fiducial nuclear saturation density) for the model GM3. Each is shown for magnetic field strengths of $B^* = 0$, 10^5, and 10^6. $P_f = B^2/8\pi$ is the pressure due to magnetic field stress for the value $B^* = 10^5$. The inset shows P_m as a function of the matter energy density ε_m. In the right panels results for leptons are shown by dashed lines while those for baryons are shown by solid lines.

The cases $B^* = 0$ and $B^* = 10^5$ are nearly indistinguishable, except for densities less than nuclear density ($u < 1$), where "cavitation" due to Landau quantization occurs. This effect has been discussed in Ref. [3] and earlier work (cf., Refs. [5, 6]). However, the structure of a magnetized neutron star will be mostly affected by contributions from the magnetic field stress, $P_f = B^2/8\pi = 4.814 \times 10^{-8} B^{*2}$ MeV fm^{-3}, which greatly exceeds the matter pressure P_m at all relevant densities for $B^* \geqslant 10^5$, as shown in Fig. 1 for $B^* = 10^5$.

Hyperons appear near twice nuclear density for $B^* \leqslant 10^5$ in this model. For $B^* > 10^5$ ($B > 5 \times 10^{18}$ G), the same value needed to noticeably affect the matter pressure and nucleon abundances, significant effects on hyperon threshold densities and abundances are apparent. Landau quantization increases the proton abundance, and hence the electron concentration due to charge neutrality. Therefore, $\mu_e = \mu_n - \mu_p$ is increased. However, at fixed baryon density, the neutron abundance must then decrease, which significantly lowers μ_n to a greater extent than $\mu_n - \mu_p$ is in-

creased. The net effect is a suppression of hyperons. In particular, note that $\mu_{\Sigma^-} = 2\mu_n - \mu_p$ and $\mu_\Lambda = \mu_n$.

It should also be noted that, compared to the case without hyperons (cf. Ref. [3]), the pressure is reduced for all field strengths, as is the nucleon effective mass. The magnitude of the nucleon effective mass can be important in determining the chemical potentials, as shown below.

We have verified that the qualitative effects of large fields on the composition, presure and effective mass are similar for the other three models considered, in the case that only Landau quantization is considered. The relative suppression of individual hyperons varies, however; for example, in models GM2 and ZM the Λ and Σ^- threshold densities reverse at large fields relative to GM1 and GM3. Importantly, however, the value $B^* \sim 10^5$ represents a threshold for field effects to become significant, independently of the EOS.

The inclusion of anomalous magnetic moments produces even larger suppressions of hyperons, as displayed in Fig. 2 for the baseline model GM3. One can qualitatively understand this trend by considering
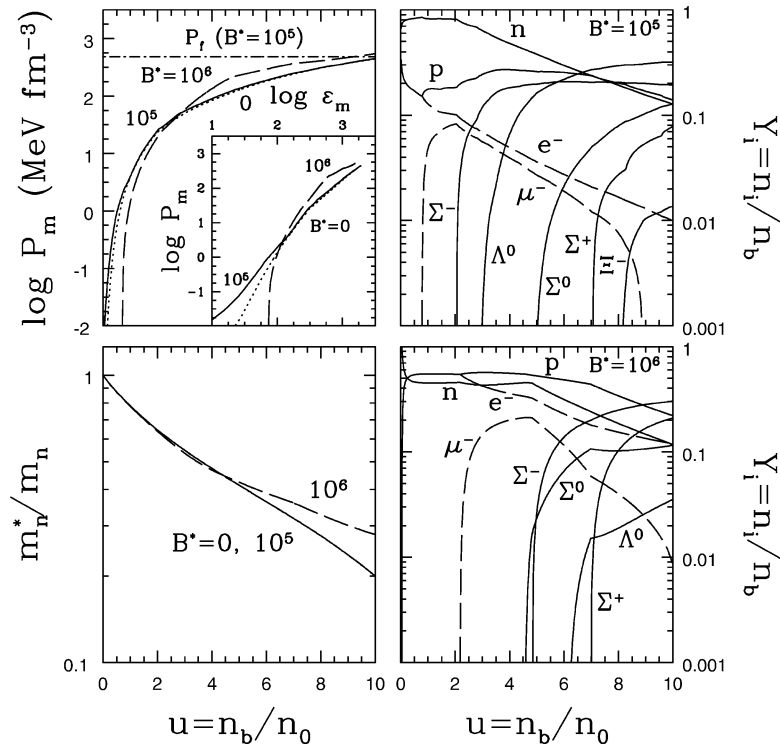

Fig. 2. Same as Fig. 1, but with magnetic moment interactions included.

the effects of magnetic moments on the baryon chemical potentials, and then examining the effects on the threshold of the first hyperon to appear. At low temperatures, the chemical potentials can be identified with the Fermi levels of the baryonic energy spectra. The energy spectrum for charged baryons is given by [3]

$$
\begin{aligned}
E_{b,n,s} &= \sqrt{k_z^2 + \left(\sqrt{m_b^{*2} + 2\nu q_b B} + s\kappa_p B\right)^2} \\
&\quad + g_{\omega_p}\omega^0 + t_{3_b} g_{\rho_p}\rho^0 \\
&\simeq m_b^* + \frac{k_z^2}{2m_b^*} + \frac{\nu q_b B}{m_b^*} + s\kappa_b B + g_{\omega_b}\omega^0 \\
&\quad + t_{3_b} g_{\rho_b}\rho^0,
\end{aligned}
\tag{5}
$$

where the quantity $\nu = n + s/2 + 1/2$ characterizes the so-called Landau level with n and s (± 1) being the principle quantum number and "spin" quantum number respectively, and t_{3_b} is the isospin projection of baryon b. The quantities ω^0 and ρ^0 are mean field solutions of the field equations corresponding to Eq. (3) (cf. Ref. [3]). The rightmost expression is valid in the nonrelativistic limits $k_z^2 \ll m_b^{*2}$, $2\nu|q_b|B \ll m_b^{*2}$ and $(\kappa_b B)^2 \ll m_b^{*2}$, which are appropriate for the conditions of interest. Similarly, the energy spectrum of neutral baryons is given by

$$
\begin{aligned}
E_{b,s} &= \sqrt{k_z^2 + \left(\sqrt{m_b^{*2} + k_x^2 + k_y^2} + s\kappa_b B\right)^2} \\
&\quad + g_{\omega_b}\omega^0 + t_{3_b} g_{\rho_b}\rho^0 \\
&\simeq m_b^* + \frac{k^2}{2m_b^*} + s\kappa_b B + g_{\omega_b}\omega^0 + t_{3_b} g_{\rho_b}\rho^0.
\end{aligned}
\tag{6}
$$

For both charged and neutral baryons, the chemical potentials of nearly degenerate systems are set by the lowest energy spin state. The contribution to neutral baryon energies, and to their chemical potentials, due to the anomalous magnetic moment is therefore $-|\kappa_b|B$ in Eq. (6). The situation of charged baryons is more complicated, because of the additional contribution due to the Dirac moment. However, given that the value of n from Landau quantization generally exceeds $|\kappa_b|/\mu_b$, the shift in charged baryon chemical potentials is not as significant as it is for neutral baryons. In matter containing only nucleons, the predominant effect of the anomalous magnetic moments is therefore to decrease μ_n, and thus the neutron abundance, relative to the case in which the anomalous moments are ignored (compare Figs. 1 and 2). A further

consequence is that the threshold density for the first hyperon, Σ^-, is increased since $\mu_{\Sigma^-} = 2\mu_n - \mu_p$. Although the chemical potential of the Σ^- also receives a contribution from its anomalous magnetic moment, the magnitude of the change is small compared to that due to the neutron. Note again that field strengths $B^* > 10^5$ are necessary to produce appreciable effects. We have verified that these conclusions hold for the other three EOSs we considered for the case when magnetic moments are included.

While most hyperon threshold densities are increased by the inclusion of anomalous magnetic moments, those of Σ^0 and Σ^+, the latter to a lesser extent, are decreased for $B^* > 10^5$. The complex interplay that exists when several baryons are simultaneously present makes a simple explanation difficult, however.

Finally, as noted in Ref. [3], the inclusion of magnetic moments produces an increase in pressure and effective mass at large fields ($B^* > 10^5$), due to increased baryon degeneracies [3]. These increases more than offset the reductions induced by the inclusion of hyperons.

Still to be addressed, however, is whether or not stable stellar configurations can exist in which the magnetic field is large enough ($B > 5 \times 10^{18}$ G) that the properties of matter are significantly affected by the magnetic field. One step in this direction was recently undertaken in Ref. [1], in which the limits of hydrostatic equilibrium for axially-symmetric magnetic fields in general relativistic configurations were analyzed. As discussed in detail in Ref. [2], in axially symmetric field configurations with a constant current function, the magnetic field contributes a centrifugal-like contribution to the total stress tensor. This can be understood by noting that for the artificial field geometry considered (namely, $\vec{B} \propto \hat{z}$), a superconducting fluid can move along field lines but not across them. Thus the "pressure" associated with the magnetic field will only act equatorially and not vertically. This flattens an otherwise spherical star, and for large enough fields, decreases the central (energy) density even as the mass is increased. For large enough fields, the star's stability is eventually compromised.

Hydrostatically stable configurations (of which some may not be stable to dynamical perturbations) for the GM3 EOS, both excluding and including hyperons, are shown in mass-equatorial radius space in
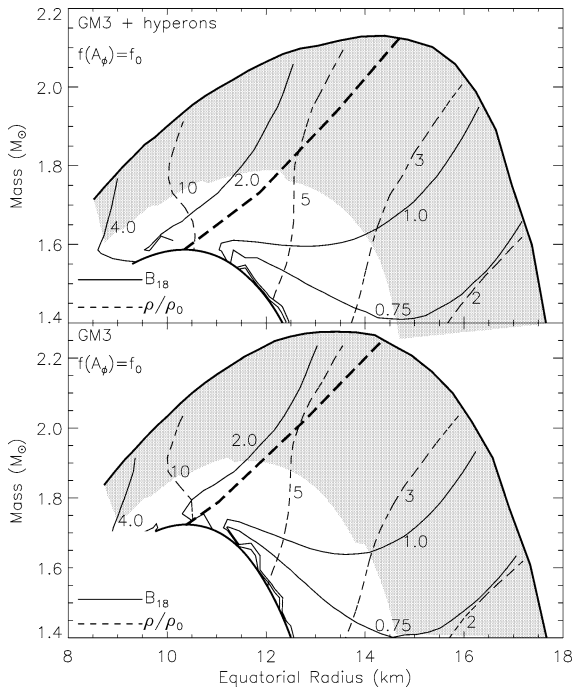
Fig. 3. Limits to hydrostatic configurations for neutron stars permeated by axially symmetric magnetic fields. The upper (lower) panel is for the EOS GM3 including (excluding) hyperons. In each panel, the lower heavy solid curve is the standard mass-radius relation for field-free stars. The upper heavy solid curve represents the largest gravitational mass possible for a given equatorial radius as the magnetic fields are increased, for the indicated current function f. The heavy dashed curve is the locus of minima of the contours of fixed baryon mass configurations: Ref. [1] suggested that this could be the limit to dynamical stability. Thin solid lines are contours of the maximum magnetic field strength in units of 10^{18} G. Similarly, thin dashed lines are contours of maximum mass-energy density in units of the energy density ρ_0 at the nuclear saturation density.

Fig. 3. The lower thick black line in each panel is the usual field-free, spherical result for the mass-radius relation. The upper thick black line represents the largest possible stable mass for a given equatorial radius as the internal field is increased. Large axially-symmetric fields tend to yield flattened configurations, and if large enough, shift the maximum densities off-center in the shaded regions in the figure. This results in toroidal shapes with low-density centers. As discussed in Ref. [1], regions to the left of the thick dashed line in this figure are likely unstable to small amplitude perturbations and hence unrealistic as stable physical configurations.

Superimposed on this figure are contours of maximum mass-energy density and magnetic field strength. For the GM3 model, hyperons appear at zero field at about twice nuclear density. Therefore, the portions of the two panels in which the maximum density is below about 3 times nuclear density are nearly identical. For the particular choice of a constant current function, but independently of the EOS, it is found that the maximum value of the magnetic field within the star cannot exceed about 3×10^{18} G, which corresponds to $B^* \sim 7 \times 10^4$. In the case of GM3, the maximum value is $B \sim 1.8 \times 10^{18}$ G. This field strength is not nearly large enough to produce appreciable effects on hyperon or nucleon compositions, with or without the inclusion of anomalous magnetic moments. The dominant effect of the field arises through the magnetic field stress, which effectively dominates the matter pressure below a few times nuclear saturation density, depending on the field's orientation. Whether other choices of current functions, or the relaxation of the condition of axial symmetry, will alter these conclusions is not clear, as the answer will likely depend on the detailed nature of the field configurations considered.

To date only a few cases of spatially varying current functions have been explored [2], but these have all been limited to axial symmetry. Furthermore, the cases explored have relatively small spatial gradients so that the ratio of the maximum field to the average field within the star is not large. It might be that the shapes of the stars will significantly change with a different field geometry. It is even possible to imagine a disordered field where $\langle B^2 \rangle$ is significantly larger than $\langle \vec{B} \rangle^2$. In this case the pressure will be dominated by fluctuations in the field, but the stars will tend to be spherical. It is possible that strong magnetic fields may be held in the core for periods much longer than the ohmic diffusion time due to interactions between the magnetic flux tubes and the vortex tubes expected to be present in a superconducting, superfluid, rotating neutron star [17]. Therefore, although the results to date imply that average fields within a neutron-star cannot exceed $1–3 \times 10^{18}$ G before stability is compromised, the value of the maximum possible field at any point within the star is undetermined. As a result, it is possible that the effects of magnetic fields upon the equation of state or particle composition will be important in some magnetic field geometries.

Acknowledgements

References

[1] C.Y. Cardall, M. Prakash, J.M. Lattimer, Astrophys. J. 554 (2001) 322.

[2] M. Bocquet, S. Bonazzola, E. Gourgoulhon, J. Novak, Astron. Astrophys. 301 (1995) 757.

[3] A. Broderick, M. Prakash, J.M. Lattimer, Astrophys. J. 537 (2000) 351.

[4] D. Lai, S. Shapiro, Astrophys. J. 383 (1991) 745;
For a recent review, see: D. Lai, Rev. Mod. Phys. 73 (2001) 629.

[5] S. Chakrabarty, Phys. Rev. D 54 (1996) 1306.

[6] S. Chakrabarty, D. Bandyopadhyay, S. Pal, Phys. Rev. Lett. 78 (1997) 2898.

[7] Y.F. Yuan, J.L. Zhang, Astrophys. J. 525 (1999) 950.

[8] D.E. Groom et al., Particle Data Group Collaboration, Eur. Phys. J. C 15 (2000) 1.

[9] N.K. Glendenning, S.A. Moszkowski, Phys. Rev. Lett. 67 (1991) 241.

[10] R. Knorren, M. Prakash, J.M. Lattimer, Phys. Rev. C (1995) 1855.

[11] J. Schaffner, I.N. Mishustin, Phys. Rev. C 53 (1996) 1416.

[12] J. Boguta, A.R. Bodmer, Nucl. Phys. A 292 (1977) 413.

[13] J. Zimanyi, S.A. Moszkowski, Phys. Rev. C 42 (1990) 1416.

[14] N.K. Glendenning, Phys. Lett. B 114 (1982) 392.

[15] N.K. Glendenning, Astrophys. J. 293 (1985) 470.

[16] M. Prakash, J.R. Cooke, J.M. Lattimer, Phys. Rev. D 52 (1995) 661.

[17] M. Ruderman, Millisecond pulsars: a decade of surprise, in: A.S. Fruchter, M. Tavani, D.C. Backer (Eds.), ASP Conf. Ser., Vol. 72, Astronomical Society of the Pacific, San Francisco, CA, 1995, p. 277.